Journal of Alloys and Compounds 509 (2011) 5773–5776

Contents lists available at ScienceDirect

Journal of Alloys and Compounds

journal homepage: www.elsevier.com/locate/jallcom

$Tb_{0.3}Dy_{0.7}Fe_{1.92}$ nanoflakes prepared by surfactant-assisted high energy ball milling

Liyun Zheng[a,b,*], Wanfeng Li[b], Baozhi Cui[b], George C. Hadjipanayis[b]

[a] School of Mechanical and Electrical Engineering, Hebei University of Engineering, Handan, Hebei 056038, PR China
[b] Department of Physics and Astronomy, University of Delaware, Newark, Delaware 19716, USA

ARTICLE INFO

Article history:
Received 20 December 2010
Received in revised form 15 February 2011
Accepted 16 February 2011
Available online 23 February 2011

Keywords:
Oleic acid
Rare earth alloys and compounds
Terfenol

ABSTRACT

$Tb_{0.3}Dy_{0.7}Fe_{1.92}$ nanoflakes with larger specific surface and higher resistance to oxidation have been prepared by high energy ball milling (HEBM) with oleic acid. The morphology, structure and magnetic properties of $Tb_{0.3}Dy_{0.7}Fe_{1.92}$ have been investigated using scanning electron microscopy, transmission electron microscopy, X-ray diffraction and vibrating sample magnetometry, respectively. The experimental results showed that the as-made samples had sustained little oxidation after surfactant-assisted HEBM suggesting that oleic acid was efficient to protect the powders from oxidation. These $Tb_{0.3}Dy_{0.7}Fe_{1.92}$ nanoflakes have great potential to be used for the preparation of high performance Terfenol composites with reduced eddy current heating.

1. Introduction

The giant magnetostrictive material Terfenol-D with the cubic Laves phase was first developed by the Naval Surface Warfare Center in the early 1970s [1]. It exhibits large magnetostriction, high Curie temperature, large magneto-mechanical coupling coefficient and rapid frequency response. This material has shown great potential in applications where operating frequencies do not exceed ~10 kHz [2]. The main disadvantages with Terfenol-D are the frequency limitation due to eddy current losses and the difficulty in machining and fabricating devices owing to its brittleness. Considerable efforts have been taken to solve these problems and develop magnetostrictive composites of Terfenol-D and nonmagnetic polymer [3–9]; such composites possess high resistance and high tensile strength. Duenas and Carman [8] investigated the effects of particle size and particle size distribution on magnetostrictive and magnetoelastic strain response. They found that optimized packing of the bimodal particle distribution has a significant effect on response as well as the minimization of demagnetizing effects. However, the Terfenol-D reported in these studies had a particle size in the micrometer scale. The only reported study that employed wet mechanical milling to reduce the particle size of Terfenol-D particles [10] and form nanocomposites was unsuccessful because the $Tb_{0.3}Dy_{0.7}Fe_{1.97}$ had decomposed and the rare earth elements in it were oxidized after wet mechanical milling.

Surfactant-assisted high energy ball milling (HEBM) has been shown to have a major effect on particle size, structure, morphology and magnetic properties of magnetic materials [11–13]. So far, there were no reports on the use of the surfactant-assisted HEBM technique to prepare Terfenol-D powders. In this work, we have prepared $Tb_{0.3}Dy_{0.7}Fe_{1.92}$ nanoflakes using oleic acid (OA) as surfactant and studied the influence of OA on the sample morphology and magnetic properties. It is interesting to note that OA was efficient not only in the reduction of grain size but also in preventing the oxidation of $Tb_{0.3}Dy_{0.7}Fe_{1.92}$.

2. Experimental details

$Tb_{0.3}Dy_{0.7}Fe_{1.92}$ ingot with an average grain size of approximately 50 μm was prepared by arc-melting using pure metals. The ingots were sealed into quartz ampoules, after evacuating to 10^{-6} Torr and backfilling with Ar, and annealed at the 1100 °C for 24 h. The annealed alloy with an average grain size of more than 300 μm was crushed, ground down to 200 μm and then milled with a SPEX 8000 M mill. The sample was milled for 5, 8 and 15 h with balls that were different in diameter. A ball-to-powder weight ratio of 10:1 was used. Heptane (99.8%) was used as the milling medium and OA (90%) as the surfactant. The amount of surfactant used in the experiments was 15 wt% and 50 wt% by weight of the starting powder.

The structure of the milled powders was examined with a Rigaku X-ray diffractometer (XRD) using Cu K_α radiation and analyzed by the Rietveld method using the PDXL program. Microstructure and morphology of the samples were investigated using a scanning electron microscope (SEM, JEOL JSM-6335F) and a transmission electron microscope (TEM, JEOL JEM-3010). Samples for TEM were prepared by letting the diluted slurry dry on carbon coated copper grids. Magnetic properties were measured using a vibrating sample magnetometer with the maximum field of 20 kOe on field-aligned powder samples embedded into wax. The VSM data were corrected by 10 wt.% surfactant that was remained in the flakes.

* Corresponding author at: Department of Physics and Astronomy, University of Delaware, 217 Sharp Lab, Newark, Delaware 19716, USA. Tel.: +1 302 5595739; fax: +1 302 8311637.
E-mail address: zheng@udel.edu (L. Zheng).

0925-8388/$ – see front matter © 2011 Elsevier B.V. All rights reserved.
doi:10.1016/j.jallcom.2011.02.092

3. Results and discussion

Fig. 1 shows the morphology of $Tb_{0.3}Dy_{0.7}Fe_{1.92}$ powders after HEBM for 8 h in heptane with and without OA. It can be seen that the majority of the $Tb_{0.3}Dy_{0.7}Fe_{1.92}$ powders ball milled *with* OA became flakes with a thickness in the range from 100 nm to 300 nm and a length in the range from 1 μm to 10 μm; some powders were in the shape of equiaxed particles. All the powders ball milled in

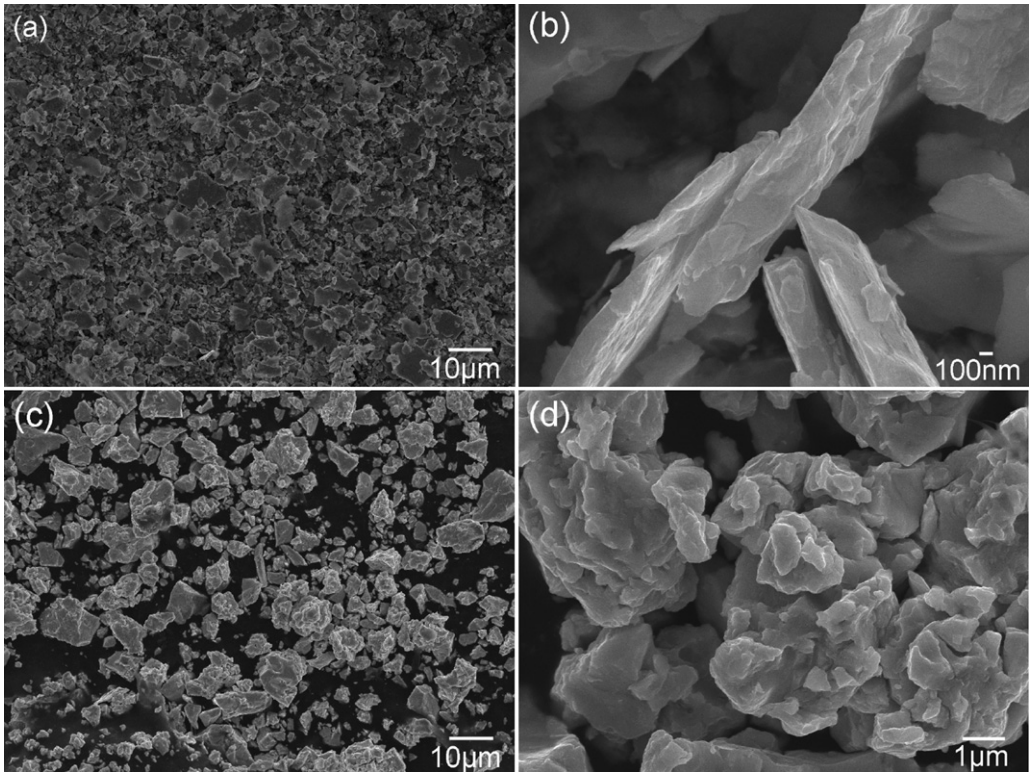

Fig. 1. SEM images of $Tb_{0.3}Dy_{0.7}Fe_{1.92}$ after HEBM for 8 h (a and b) with 15 wt% OA, (c and d) without OA.

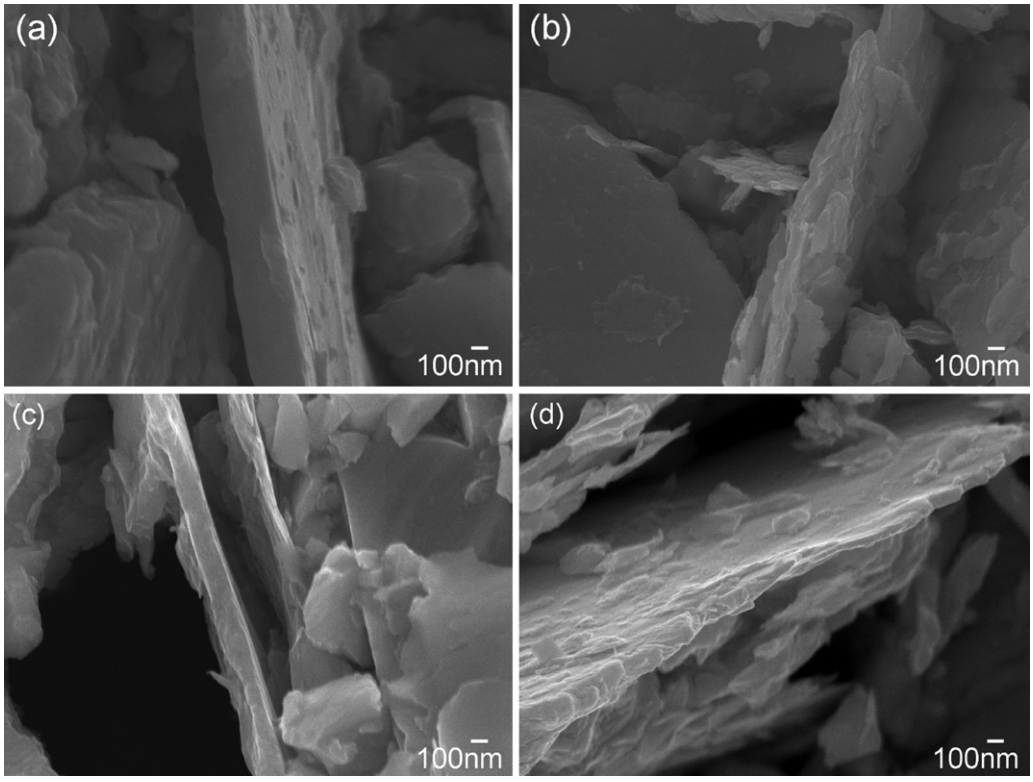

Fig. 2. SEM images of $Tb_{0.3}Dy_{0.7}Fe_{1.92}$ after HEBM for (a) 5 h, (b) 15 h with 15 wt% OA, and (c) 5 h and (d) 15 h with 50 wt% OA.

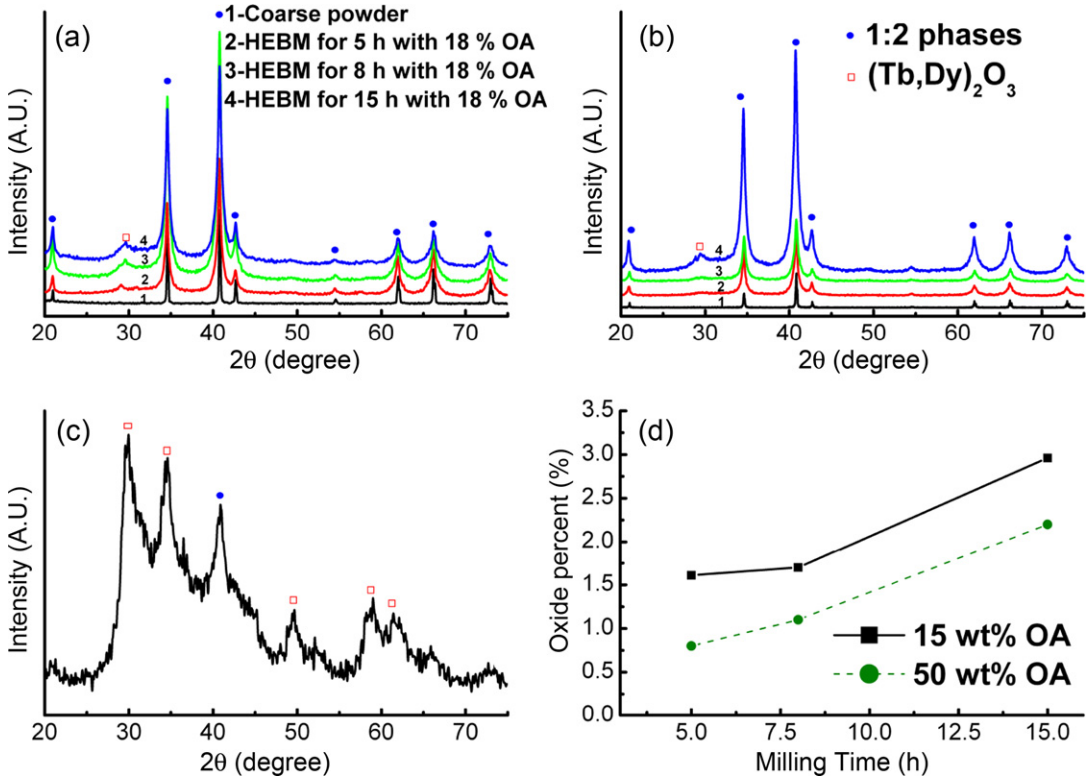

Fig. 3. The XRD patterns of the $Tb_{0.3}Dy_{0.7}Fe_{1.92}$ powders before and after HEBM with (a) 15 wt% OA and (b) 50 wt% OA, (c) for 8 h without OA and (d) the content of oxide phase after HEBM with different OA contents. (For interpretation of the references to color in this figure legend, the reader is referred to the web version of the article.)

heptane *without* OA appeared to have an equiaxed particle shape (Fig. 1c and d).

With 50 wt% OA, the majority of powders also appeared to have a flake shape; a small amount of particles is also observed (Fig. 2). The flakes produced with 50 wt% OA were thinner than those produced with 15 wt% OA. According to Fig. 2, the thickness of the flakes varied from approximately 400 nm to 50 nm after HEBM for 5 and 15 h with 15 wt% OA, respectively, and 150 nm to 50 nm after HEBM for 5 and 15 h with 50 wt% OA, respectively. Thus, by increasing both the milling time and the amount of OA the flakes become thinner.

Fig. 3 shows the XRD patterns of $Tb_{0.3}Dy_{0.7}Fe_{1.92}$ powders before and after HEBM. The pronounced presence of the oxide phase $(Tb,Dy)_2O_3$ in Fig. 3a–c indicates that a dramatic oxidation occurred when the $Tb_{0.3}Dy_{0.7}Fe_{1.92}$ powder was milled without the protection of OA. From Fig. 3d, the amount of oxide phase in the milled powders, determined through XRD–Rietveld analysis, decreased with increasing OA. These results indicate that the surfactant protects efficiently the $Tb_{0.3}Dy_{0.7}Fe_{1.92}$ from oxidation during the HEBM process. The average crystallite size of the $Tb_{0.3}Dy_{0.7}Fe_{1.92}$ powders after HEBM for 5, 8 and 15 h with 15 wt% OA was estimated from Scherrer's formula and found to be approximately 17, 15 and 12 nm, respectively; the sizes of those with 50 wt% OA were approximately 21, 15 and 11 nm, respectively. However, in the case of HEBM without OA, the $Tb_{0.3}Dy_{0.7}Fe_{1.92}$ powders had no protection of surfactant during the HEBM process and had a strong tendency to oxidize due to the much larger fresh surface formed during HEBM.

Fig. 4 shows a high resolution transmission electron microscope (HRTEM) image of $Tb_{0.3}Dy_{0.7}Fe_{1.92}$ after high energy ball milling for

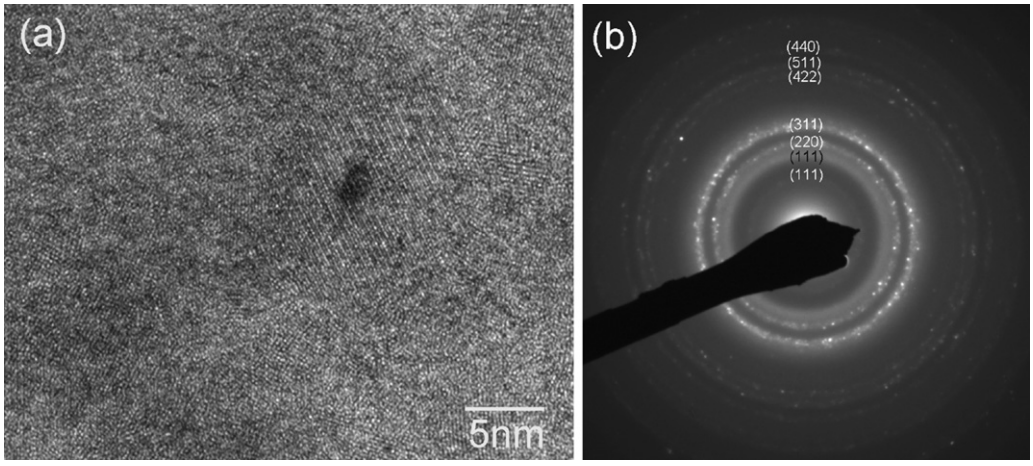

Fig. 4. (a) HRTEM image and (b) SAD pattern of $Tb_{0.3}Dy_{0.7}Fe_{1.92}$ after HEBM for 5 h with 15 wt% OA.

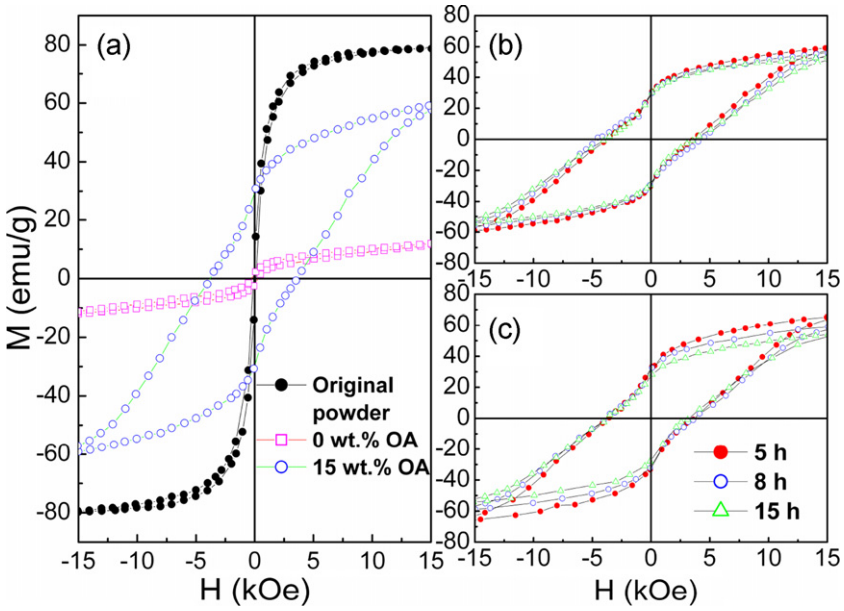

Fig. 5. Magnetic properties of the $Tb_{0.3}Dy_{0.7}Fe_{1.92}$ powders (a) before and after HEBM for 8 h with 15 wt% OA and without OA, (b) HEBM for different times with 15 wt% OA, and (c) HEBM for different times with 50 wt% OA. (For interpretation of the references to color in this figure legend, the reader is referred to the web version of the article.)

5 h with 15 wt% OA. The micrograph reveals that the grain size in the nanoflake is approximately 16 nm, which is consistent with the size calculated from XRD data. It indicates that poly-nanocrystalline nanoflakes with an average grain size of 16 nm were eventually formed via the single crystal microparticles, microflakes and then single-crystal submicro flakes during the surfactant-assisted HEBM process, which is similar to the formation mechanism of $SmCo_5$ nanoflakes during the surfactant-assisted HEBM as described in Ref. [14]. For the flake with a length in the range of 1–10 μm, it composed of approximately 1.6×10^4–1.6×10^6 grains. After analysis of the selected area diffraction (SAD), it is found that the flake consisted of the 1:2 phase (white indexes in Fig. 4b) and the $(Tb,Dy)_2O_3$ phase (black font indexes in Fig. 4b), which is consistent with the XRD analysis results.

Fig. 5a shows the magnetic properties of $Tb_{0.3}Dy_{0.7}Fe_{1.92}$ powders before and after HEBM for 8 h with and without 15 wt% OA. It can be seen that the $Tb_{0.3}Dy_{0.7}Fe_{1.92}$ before HEBM exhibited very small coercivity and a saturation magnetization of 79.4 emu g^{-1}. The $Tb_{0.3}Dy_{0.7}Fe_{1.92}$ alloy subjected to HEBM with 15 wt% OA developed a coercivity of 3.8 kOe and its magnetization decreased to 61.2 emu g^{-1}. This increase of coercivity may be directly associated with the reduction of grain size, since the average grain size of the as-milled sample was in the range of 15–21 nm. On the other hand, the shape anisotropy that occurs in the small scale creating preferential easy axis dependent upon shape may also contribute to the increase of coercivity. The $Tb_{0.3}Dy_{0.7}Fe_{1.92}$ sample after HEBM without OA had even a lower magnetization (13.3 emu g^{-1}) due to the oxidation.

From Fig. 5b and c, it can be seen that the saturation magnetization decreased with the increasing of milling time. But the coercivities of these powders processed with 15 wt% OA increased from 3.8 kOe to 4.6 kOe with increasing milling time and then decreased with further increasing milling time. When 50 wt% OA was used, there was no big difference between the coercivities of $Tb_{0.3}Dy_{0.7}Fe_{1.92}$ powders. The initial increase in coercivity is attributed to a grain refinement while the decrease may be mainly due to the partial oxidation of the powders.

4. Conclusions

The influence of OA during the process of $Tb_{0.3}Dy_{0.7}Fe_{1.92}$ nanoflakes has been investigated. The majority of $Tb_{0.3}Dy_{0.7}Fe_{1.92}$ powders milled with OA became nanoflakes with a thickness of 50–400 nm. The thickness became smaller with increasing milling time and the amount of surfactant. The grain sizes of $Tb_{0.3}Dy_{0.7}Fe_{1.92}$ powders after HEBM with OA were in range of 15–21 nm. The amount of oxide decreased with increasing the amount of OA.

Acknowledgments

This work is financially supported by 'The Excellent Going Abroad Experts' Training Program and 'The Talent Project' of Hebei Province (China) and by NSF DMR0302544. Dr. Liyun Zheng thank Dr. A.M. Gabay from Department of Physics and Astronomy, University of Delaware, for the discussions and suggestions.

References

[1] A.E. Clark, H.S. Belson, R.E. Strakna, J. Appl. Phys. 44 (1973) 2913.
[2] M. Fahlander, M. Richardson, Proceedings of the 10th International Workshop on Rare Earth Magnets and Their Applications, Kyoto, Part 1, 1989, p. 289.
[3] L. Sandlund, M. Fahlander, T. Cedell, A.E. Clark, J.B. Restorff, M. Wun-Fogle, J. Appl. Phys. 75 (1994) 5656.
[4] O.Y. Kwon, H.Y. Kim, S.H. Hong, D.R. Son, J. Appl. Phys. 100 (2006), 123905.
[5] J.C. Kim, O.Y. Kwon, Z.H. Lee, Appl. Phys. Lett. 84 (2004) 2130.
[6] Z.J. Guo, S.C. Busbridge, Z.D. Zhang, B.W. Wang, A.R. Piercy, J. Magn. Magn. Mater. 239 (2002) 554.
[7] H. Meng, T. Zhang, C. Jiang, H. Xu, Appl. Phys. Lett. 96 (2010), 102501.
[8] T.A. Duenas, G.P. Carman, J. Appl. Phys. 90 (2001) 2433.
[9] J. Hudson, S.C. Busbridge, A.R. Piercy, Sens. Actuators 81 (2000) 294.
[10] J. Tang, W. Zhao, C.J. O'Connor, S. Li, J. Alloys Compd. 250 (1997) 482.
[11] V.M. Chakka, B. Altuncevahir, Z.Q. Jin, Y. Li, J.P. Liu, J. Appl. Phys. 99 (2006), 08E912.
[12] B.Z. Cui, A. Gabay, W.F. Li, M. Marinescu, J. Liu, G.C. Hadjipanayis, J. Appl. Phys. 107 (2010), 09A721.
[13] L. Zheng, B.Z. Cui, N.G. Akdogan, W.F. Li, G.C. Hadjipanayis, J. Alloys Compd. 504 (2010) 391.
[14] B.Z. Cui, W.F. Li, G.C. Hadjipanayis, Acta Mater. 59 (2011) 563.